Adverse Event Detection (AED) System for Continuously Monitoring and Evaluating Structural Health Status

Jinsik Yun*[a], Dong Sam Ha[a], Daniel J. Inman[b] and Robert B. Owen[c]
[a]Center for Embedded Systems for Critical Applications (CESCA)
Department of Electrical and Computer Engineering, Virginia Tech, Blacksburg, VA 24061;
[b]Center for Intelligent Material Systems and Structures (CIMSS)
Department of Mechanical Engineering, Virginia Tech, Blacksburg, VA 24061

[c]Extreme Diagnostics, Inc.
2525 Arapahoe Avenue
Bldg. E4 #262
Boulder CO 80302-6746

ABSTRACT

Structural damage for spacecraft is mainly due to impacts such as collision of meteorites or space debris. We present a structural health monitoring (SHM) system for space applications, named Adverse Event Detection (AED), which integrates an acoustic sensor, an impedance-based SHM system, and a Lamb wave SHM system. With these three health-monitoring methods in place, we can determine the presence, location, and severity of damage. An acoustic sensor continuously monitors acoustic events, while the impedance-based and Lamb wave SHM systems are in sleep mode. If an acoustic sensor detects an impact, it activates the impedance-based SHM. The impedance-based system determines if the impact incurred damage. When damage is detected, it activates the Lamb wave SHM system to determine the severity and location of the damage. Further, since an acoustic sensor dissipates much less power than the two SHM systems and the two systems are activated only when there is an acoustic event, our system reduces overall power dissipation significantly. Our prototype system demonstrates the feasibility of the proposed concept.

Keywords: structural health monitoring, SHM, impedance-based method, Lamb wave method, acoustic emission

1. INTRODUCTION

Structural Health Monitoring (SHM) is the science and technology of monitoring and assessing the condition of aerospace, civil, and mechanical infrastructures using a sensing system integrated into the structure. SHM is capable of detecting, locating, and quantifying various types of damage such as cracks, holes, corrosion, delamination, and loose joints, and can be applied to various kinds of infrastructures such as buildings, railroads, windmills, bridges, and aircraft. To detect or locate various types of defects, it necessitates an SHM system to employ different SHM methods [1]. However, most existing SHM systems employ only one type of SHM methods targeting specific damages [2],[3]. To cover different types of damages, we need multiple such SHM systems, resulting in an increased form factor, power consumption, and cost.

A variety of approaches to SHM have been proposed and investigated. The impedance-based method based on using piezoelectric wafers, such as PZT (Lead Zirconate Titanate), is proven to be effective for in situ local damage detection [3]. An impedance-based SHM system performs three major operations: excitation signal generation, sensing the response signal, and damage assessment. The excitation signal for existing SHM systems is typically a sweeping sinusoidal signal, which is generated with a digital-to-analog converter (DAC). The response signal is captured by an analog-to-digital converter (ADC) and processed by a digital signal processing (DSP) chip or microcontroller unit (MCU). Existing impedance-based systems are complicate and power hungry. To address the problems, we investigated

a new impedance-based SHM method, which performs SHM operations in the digital domain [3]-[5]. Our system excites a PZT patch with a train of rectangular pulses instead of a sinusoidal signal, which eliminates a DAC. Our system senses only the phase, not the magnitude, of the response signal to eliminate an ADC. Therefore, our system is much simpler in hardware and dissipates far less power.

One limitation of the impedance method is its inability to locate the defect, and the Lamb wave propagation method addresses the limitation. The Lamb wave method launches an elastic wave through the structure. The changes in both wave attenuation and reflection are sensed to detect and locate damage on surfaces [6],[7]. We investigated a power efficient Lamb wave method, which eliminates a power hungry ADC [8]. We also investigated integration of both the impedance-based and Lamb wave methods into a single SHM system [1]. A Hanning windowed sinusoidal signal is generated to excite a Lamb wave for our integrated system. A Hanning windowed sinusoidal signal has a small frequency bandwidth [9], so the generated Lamb waves are limited to the fundamental mode. We applied a discrete wavelet transform to the sensed response, which reduces processing complexity and the memory requirement compared with other transformations such as FFT (Fast Fourier Transform). Since both the impedance and the Lamb wave methods can share a processor and piezoelectric patches, our integrated SHM system reduces the form factor and the power dissipation.

High power consumption of SHM systems is problematic for many SHM applications including spacecraft. In this paper, we present a low power SHM system, named *Adverse Event Detection* (AED), in which an acoustic sensor is added to our integrated SHM system employing both the impedance-based and the Lamb wave methods. Our AED system intends for spacecraft whose damage is often due to collision of meteorites or space debris. With these three health-monitoring methods, we can determine the presence, location, and severity of damage. The acoustic sensor continuously monitors acoustic events such as collision of meteorites. If an acoustic sensor detects an impact, it activates the impedance-based SHM system. The impedance-based system determines if the impact incurred damage. When damage is detected, the impedance-based system activates the Lamb wave SHM system to determine the severity and location of the damage. An acoustic sensor continuously monitors acoustic events, while the impedance-based and Lamb wave SHM systems are in sleep mode. The two SHM systems are activated only when there is an acoustic event. As an acoustic sensor dissipates much smaller power compared with the impedance-based and the Lamb wave SHM systems, use of an acoustic sensor reduces overall power dissipation of the system.

The paper is organized as follows. Section 2 reviews briefly the impedance-based and the Lamb wave-based SHM systems. Section 3 describes the operation, architecture, and prototype of our AED system. Section 4 presents experimental results, and Section 5 summarizes our work.

2. PRELIMINARIES

We review the impedance-based and the Lamb wave SHM systems employed in our AED system in this section. We also describe the acoustic sensor used for our system.

2.1 Impedance-based SHM system

Analog Device, Inc. introduced an impedance analyzer chip AD5933, which dissipates about 30 mW. The chip includes a DAC to generate an excitation signal up to 100 kHz, a 12-bit ADC, and supports on-chip FFT operation. Park et al. integrated this chip with a microcontroller ATMega128 and an XBee wireless transceiver [10]-[12]. Researchers from Los Alamos National Lab have worked on a series of wireless SHM sensor systems embedded with Analog Device's impedance analyzer chips AD5933 for years and developed the third generation of the sensor system called Wireless Impedance Device (WID-3) in 2009 [13]-[15].

Our team also developed a series of impedance-based SHM systems using Texas Instrument DSP and low-power microcontroller unit (MCU) evaluation boards [3]-[5]. We employed three methods to reduce power consumption of our impedance-based SHM systems. These three methods are reviewed in the following sections.

- **On-board Data Processing:**

The major source of power consumption for a wireless sensor node is the radio. For example, a microcontroller unit MSP430 from Texas Instruments used for our SHM sensor node in [3] dissipates 3 mW under a low-power operation mode, while a low-end radio CC2500 from Texas Instruments embedded in the sensor node dissipates 65 mW during transmission. So, it is essential to reduce the radio transmission time for a low-power wireless SHM sensor node. We adopted an on-board data processing approach for our SHM sensor node in [3], which processes the data on the board and sends only the final outcome (healthy or damaged) of the SHM operation to the control center.

- **Elimination of a DAC for generation of an excitation signal**

A sinusoidal signal sweeping a certain frequency range is usually used to excite a PZT patch for the impedance-based method. Sampled values of a sinusoidal signal are pre-stored in a memory, and a DAC reproduces the corresponding analog signal. This method is straightforward, but it requires a DAC and a large memory space for a large frequency sweeping range. Our method is to use a rectangular pulse train rather than a sinusoidal signal. A rectangular pulse train illustrated in Figure 1 (a) has a duty cycle of 0.5, and its fundamental frequency (which is given as $1/t_p$, where t_p is the pulse period) sweeps a certain desired frequency range. The Fourier transform of a pulse train with a pulse period t_p and the duty cycle of 0.5 has odd harmonics kf_o, k=1, 3, 5 …, where $f_o = 1/t_p$. Figure 1 (b) illustrates frequency components of a pulse train with the fundamental frequency ranging from 40 kHz to 50 kHz. The magnitude of the third harmonic is about 33 percent of the fundamental frequency, and the fifth one about 20 percent.

A rectangular pulse train is digital, and hence a processor can directly generate such a signal. Hence, a DAC is eliminated for our system to save power. One potential issue is existence of harmonics on the signal. Since both the baseline and measured impedance profiles are under the subject of the same frequency terms, the sensitivity for the detection metric may not be affected by harmonics. Our experimental results in [4] reveal that use of a rectangular pulse train does not incur any noticeable deterioration of the performance for the impedance method.

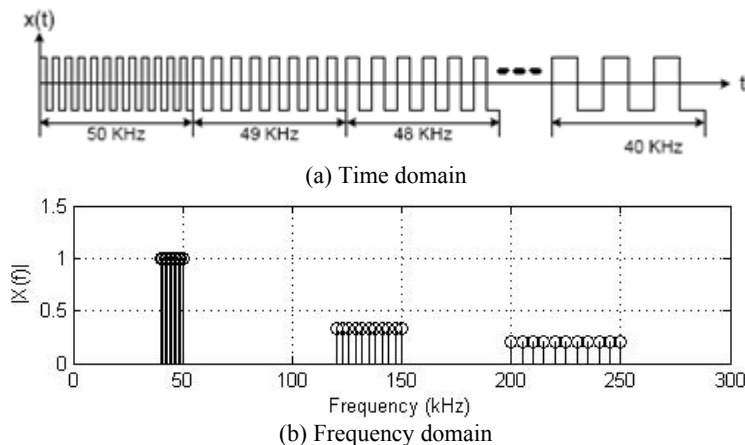(a) Time domain

(b) Frequency domain
Figure 1. Rectangular pulse train

- **Elimination of an ADC for response signal sensing**

Existing methods, such as one employed by Analog Device's impedance analyzer chips, sample the response signal using an ADC and performs an FFT to extract the impedance component of the frequency. A typical ADC used for an SHM system consumes large power, possibly next to a radio and a processor, and FFT is also computationally intensive to increase power dissipation. Our method is to eliminate an ADC and the FFT operation by sensing the phase, not the magnitude, of the response signal.

The electrical admittance is expressed as $Y(jf) = G(f) + jB(f)$, where $G(f)$ and $B(f)$ are conductance and susceptance terms, respectively. It is known that the conductance term of a PZT patch is more sensitive to damage [16]. Let $G_{base}(f)$

denote the baseline conductance obtained from a healthy structure and $G_{SUT}(f)$ be the conductance of a structure under test (SUT). The difference of the two conductance terms $G_{base}(f) - G_{SUT}(f)$ is used for existing impedance-based SHM systems to detect damage. Assuming all parameters are constant, our earlier work showed that

$$G_{base}(f) - G_{SUT}(f) \approx C \sin[\phi_{base}(f) - \phi_{SUT}(f)]$$ (1)

where C is a constant, and $\phi_{base}(f)$ and $\phi_{SUT}(f)$ are the phase of the baseline admittance and the SUT admittance, respectively [17]. Expression (1) suggests that the difference of the phases, instead of the conductance $G(f)$'s, can be sensed for the impedance method.

The phase of an admittance (f) for a frequency f can be expressed as in (2), where $T_d(f)$ is the time difference between the voltage and the current:

$$\phi(f) = 2\pi f \times T_d(f)$$ (2)

When both the voltage and current are represented as binary signals, the time difference $T_d(f)$ of the two signals is obtained using an exclusive-OR (XOR) operation as illustrated in Figure 2. For details, refer to [3].
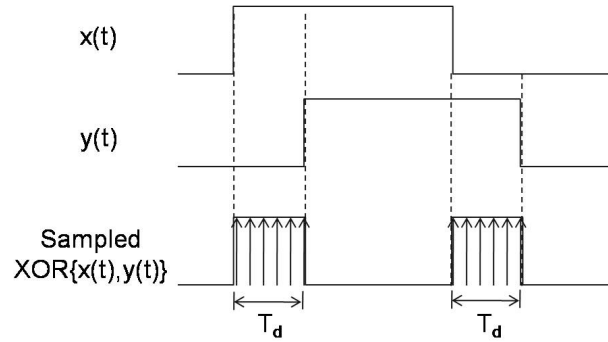

Figure 2. Phase difference measured by sampling the output of the XOR operation

- **Damage Metric**

The damage metric (DM) for our system is defined as a normalized absolute sum-of-differences between the phase profiles of the baseline and of the SUT given by

$$DM = \frac{\sum_{f_i=f_l}^{f_h} |\phi_{base}(f_i) - \phi_{SUT}(f_i)|}{M(f_l, f_h)}$$ (3)

where $M(f_l, f_h)$ is the number of frequency points from the lowest frequency f_l to the highest frequency f_h. The DM of a SUT is compared against a threshold value, whose value may be set based on field experience. If the DM is lower than the threshold value, the SUT is considered healthy. Otherwise, it is damaged. It is important to note that fixed-point calculations without involving multiplications or division are sufficient for Expression (3) provided $M(f_l, f_h)$ is set to power of 2. So, a simple fixed-point processor, rather than a floating-point processor, can be used for our SHM system to save power. Adoption of a more sophisticated DM is possible for our system to improve the SHM performance, but it is not the objective of our system.

2.2 Lamb wave SHM system

A Lamb wave SHM system uses a piezoelectric transducer, specifically a PZT patch, to launch an elastic wave into a structure, and the response signal is sensed by the same PZT patch or another attached somewhere else on the structure

[6],[7]. A self-contained Lamb wave system typically comprises three functional blocks: a signal actuation block, a signal sensing block, and a signal processing block. The signal actuation block is comprised of a DAC, which generates an analog signal from a waveform stored in memory. This analog signal is then amplified and applied to a PZT patch attached to the structure. The response signal picked up by a PZT patch is usually amplified, sampled, and digitized by an ADC. Finally, the signal processing block processes the received response, and the received signal is compared against a baseline to determine whether or not damage exists in the system. A signal processing block typically employs a general purpose processor, a DSP chip, or an MCU.

To design a Lamb wave system, it is important to determine an optimal driving frequency for the structure under test. The excitation waveform also plays an important role in determining the effectiveness of a Lamb wave system. One of the most commonly employed excitation waveforms is a tone burst sine wave with a Hanning window, which is a raised-cosine with a roll-off factor of 1. Because a Hanning windowed sinusoid has low bandwidth, the generated Lamb waves are limited to their fundamental modes [9]. Figure 3 shows an excitation waveform in both the time domain and the frequency domain.

(a) Excitation Waveform in time domain

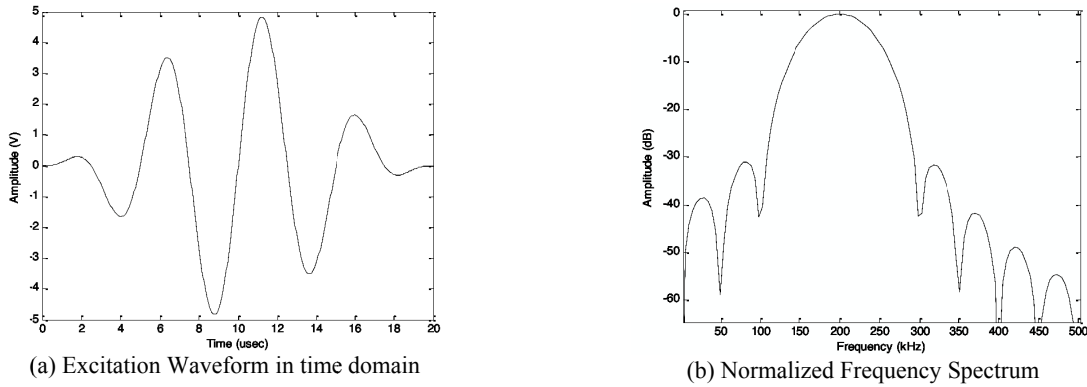(b) Normalized Frequency Spectrum

Figure 3. 200 kHz excitation waveforms

A discrete wavelet transformation (DWT) is typically used to reduce noise [18],[19]. DWT is a special case of the wavelet transform that provides a compact representation of a signal in time and frequency, and it can be computed efficiently. DWT is defined in the following expression:

$$W_\Psi(j,k) = \sum_j \sum_k s(n) 2^{-j/2} \Psi_{j,k}(2^{-j}n - k) \tag{4}$$

where $\Psi_{j,k}$ is called as mother wavelet with finite energy. The flexibility of choosing a proper mother wavelet is one of the strongest advantages of using DWT. If we choose the mother wavelet as the excitation signal itself and the dilation coefficient $j = 0$, the DWT results in the correlation between the excitation signal and the sensed signal, which is simple to compute.

The DM used for our system is a normalized absolute sum of difference between the DWT of the baseline or reference signature and the DWT of the sensed signature from the structure under test. The DM indicates the amount of deviation of the sensed signature from the baseline. The DM increases with the damage level and is ideally zero for a structure without damage. The DM is expressed as follow:

$$DM = \frac{\sum_i \left| WT_{current}(i) - WT_{baseline}(i) \right|}{\sum_i \left| WT_{baseline}(i) \right|} \tag{5}$$

where $WT_{current}$ and $WT_{baseline}$ denote DWT of the sensed and baseline waveforms, respectively. $|x|$ denotes the absolute value of x.

2.3 Acoustic Emission Sensor

When a material structure is distorted or damaged by an external or internal force, it releases energy in the form of ultrasonic vibrations, and this phenomenon is termed acoustic emission (AE) [20]. Due to the fact that a stress causes acoustic emission, AE is also referred to as Stress Wave Emission. Since most AE sources are damage-related, detection and monitoring of these

emissions are commonly used to predict material and structural failure [21],[22]. Acoustic emissions emanating from within the structural materials can provide information about growing cracks and deformation of structures and adverse chemical reactions, such as corrosion. By analyzing AE information, small-scale damage is detectable long before failure, so that AE can be employed for non-destructive evaluation (NDE) in aeronautics, mechanical engineering, and civil infrastructure systems to find defects during structural proof tests and plant operation.

An acoustic emission sensor generates an electrical signal proportional to the AE level. An AE sensor enables detection of low level sonic and ultrasonic signals generated by impacts of meteorites or space debris for our system. Key performance parameters of an AE sensor are sensitivity, compatibility, and low power consumption for our system. We have selected an acoustic sensor PK15I from the Physical Acoustics Corporation (PAC) for our system [23]. Specifications of the AE sensor are summarized below in Table 1. The sensitivity of an AE sensor is represented as "dB ref 1V/μbar" (1 bar = 0.987 atm $\approx 10^5$ N/m^2). The unit represents the generated voltage over the reference that is 1V per 1 μbar, and a larger value represents higher sensitivity. The sensitivity of our sensor is -36 dB ref V/μbar, which means it generates $10^{-1.8}$ V under the application of pressure 1μbar. Typical AE sensors for industry applications have around -60 dB ref 1V/μbar [23],[24], and the sensitivity of highly sensitive AE sensors is around -30 dB ref 1V/μbar. Our sensor PK15I provides reasonably high sensitivity (-36 dB ref 1V/μbar) and is well suited to the repetitive laboratory tests and experiments.

Table 1: Specification of Acoustic Sensor PK15I

Dynamic	
Peak Sensitivity	-36 dB ref V/μbar
Operating Frequency	50 ~ 200 KHz
Environmental	
Temperature Range	-35 ~ 80 °C
Shock Limit	500 g
Physical	
Dimension	20.6 cm (diameter) x 27
Weight	51 g
Case Material	Stainless steel
Connector	SMA
Electrical	
Input Voltage Range	4 ~ 7 V
Operating/Max Current	5/35 mA
Internal Preamp Gain	26 dB

3. PROPOSED AED SYSTEM

We describe the operation and a prototype of our AED system in this section, which integrates an AE sensor with two SHM systems, the impedance-based and the Lamb wave.

3.1 System Operation

The objective of our AED system is to deliver an integrated structural health monitoring system, which uses acoustic emission to detect adverse impacts, the impedance method to monitor structural integrity, Lamb wave method to assess surfaces. An acoustic sensor monitors acoustic emission continuously, while the impedance-based and the Lamb wave systems are in sleep mode. When the acoustic sensor detects an impact, it wakes up the impedance-based SHM, which determines if the impact incurred damage. When damage is detected, it activates the Lamb wave SHM system to determine the severity and location of the damage. The flow chart of the AED system is shown in Figure 4.
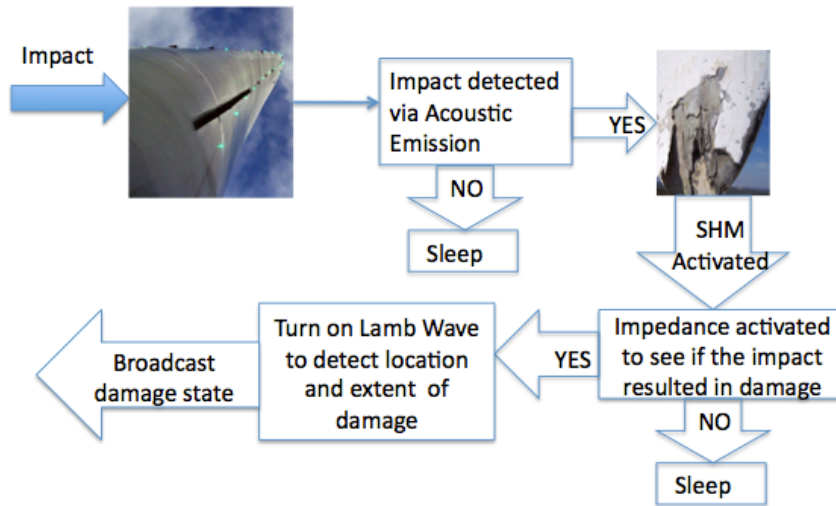
Figure 4. Flow chart of the AED system

3.2 Prototype

A prototype of our AED system is based on a TMS320F2812 DSP evaluation board from Texas Instruments [25]. TMS320F2812 is a 32-bit fixed point DSP supporting up to 150 million instructions per second (MIPS). Figure 5 (a) shows the block diagram of the AED system. The impedance-based and the Lamb wave systems share the DSP board for signal processing and control. The RS232 interface provides communication between the SHM system and a Graphical User Interface (GUI) program running on a host PC. Figure 5 (b) shows our prototype. The five blocks in Figure 5 (a) are labeled as "A" through "E" in Figure 5 (b). Figure 6 shows acoustic sensor PK151 attached to an aluminum plate, which monitors acoustic emission on the plate.

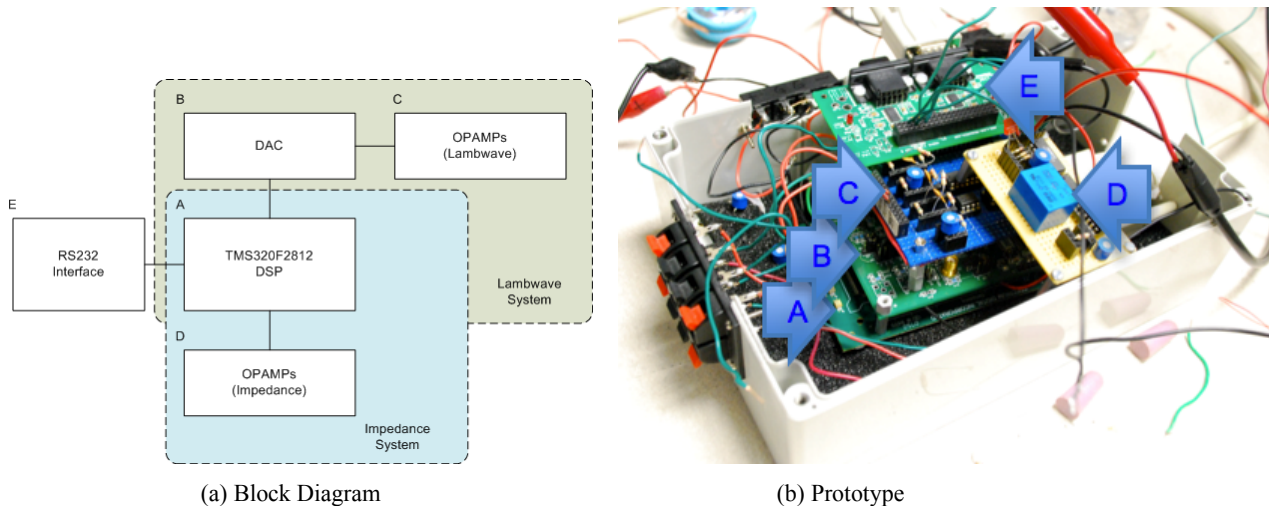(a) Block Diagram   (b) Prototype

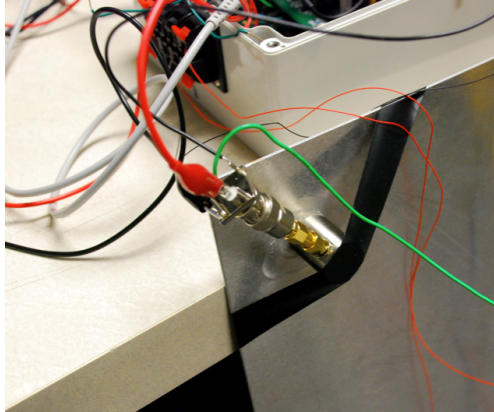Figure 5. Block Diagram and a Prototype of the AED system

Figure 6. Acoustic sensor attached on an aluminum plate

4. EXPERIMENTAL RESULTS

We present the test environment and experimental results of our AED system in this section. We use an aluminum plate as a test structure and conducted experiments with the prototype described in the above.

4.1 Test Environment

Figure 7 (a) shows two PZT patches on an aluminum plate. The PZT labeled as "1" is for the Impedance-based SHM system and called named PZT #1 hereafter, and The PZT labeled as "2" is for the Lamb wave system called PZT #2. We obtained the baseline profiles for both the impedance-based SHM system and the Lamb wave system for the health structure. Then, we made a 4″x2″ hole at six inches away from PZT #2 as shown in Figure 7 (b), and the hole emulates damage.

To emulate an adverse event on the specimen, a light stroke with a small hammer (with 1/4 lb head weight) is applied to the aluminum plate. The AE sensor generates a signal with the peak voltage of 0.5 V, which wakes up an Impedance-based SHM system.
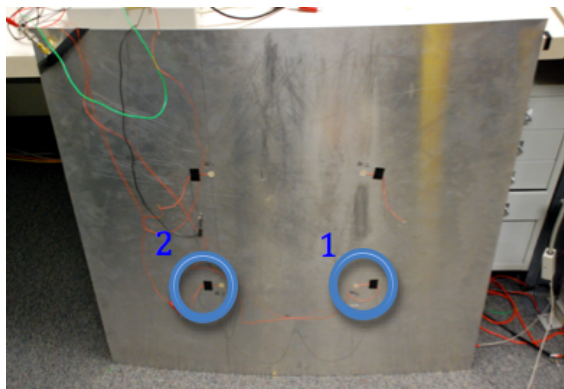
(a) Health structure

(b) Structure with damage

Figure 7. Aluminum plate as a test structure

4.2 Impedance-based SHM

We empirically obtained the excitation frequency range of 8 KHz to 150 KHz of the test structure using an impedance analyzer, in which the magnitude of the impedance has many peaks. As noted in Section 2.1, our impedance-based SHM measures the phase of the admittance. Figures 8 (a) and (b) show the phase profiles of the healthy and damaged structures, respectively. As can be seen from the two pictures, the two phase profiles are significantly different to demonstrate the effectiveness of the proposed method. The DM for our system is normalized absolute sum-of-

differences. The DM is obtained to be 29 for this particular damage and exceeds the threshold value of 10 (which was obtained through experiments) to initiate the Lamb wave system.

| (a) Healthy structure | (b) Damaged structure |

Figure 8. Phase profiles of the healthy and damaged structures

4.3 Lamb Wave SHM

The excitation signal for our system was obtained through experiment. It is a tone burst 200 KHz sine wave with a Hanning window under a raised-cosine of a roll-off factor of 1, and the waveform and its frequency spectrum are shown in Figure 3. The top waveform in Figure 9 is a wavelet-transformed baseline signal for the healthy structure measured by PZT #2. The bottom waveform in the figure is a wavelet-transformed signal for the damaged structure measured by the same PZT patch. The major difference between the two waveforms is the signal encircled in the bottom figure, which is an echo signal reflected at the perimeter of the damage hole. The arrival time of the echo signal is 56.32 μs, and the surface velocity measured for the aluminum is 0.2125 in/μs. So, the distance to the damage is obtained as 5.984 inches (= ½ × 56.32 μs × 0.2125 in/μs), which is close to the actual distance.
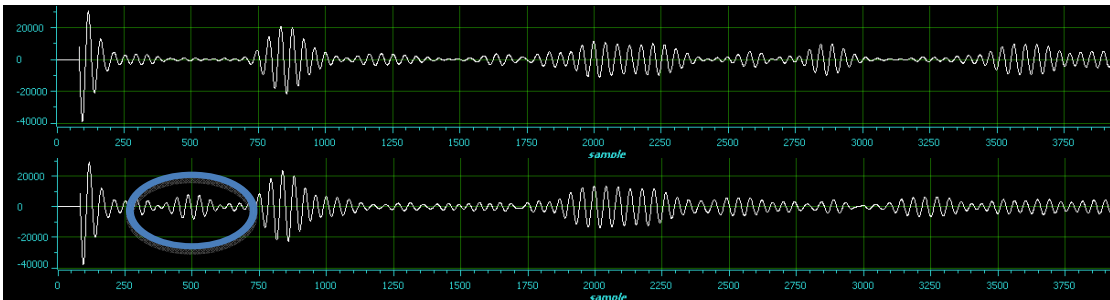

Figure 9. Wavelet transformed Lamb wave signals (a) baseline, (b) currentline

5. SUMMARY

We presented our Adverse Event Detection (AED) SHM system, which integrates an acoustic sensor, impedance-based and Lamb wave SHM systems. An acoustic sensor detects impacts, which activates the impedance-based SHM. When damage is detected by the impedance-based SHM system, it activates the Lamb wave SHM system to determine the severity and location of the damage present. An acoustic sensor continuously monitors acoustic events, while the impedance-based and the Lamb-wave SHM systems are in sleep mode. The two SHM systems are activated only when there is an acoustic event. Therefore, use of an acoustic sensor reduces overall power dissipation of our AED system.

We developed a prototype using a Texas Instruments TMS320F2812 DSP evaluation board to demonstrate the feasibility of our method. Experiment results successfully verified the proof of concept for the proposed system. The proposed method can be effective for space applications, in which meteorites and space debris may cause structural damage and low power consumption is critical.

ACKNOWLEDGEMENT

REFERENCES

[1] J.K. Kim, D. Zhou, D.S. Ha, and D.J. Inman, (2009), "A Practical System Approach for Fully Autonomous Multi-Dimensional Structural Health Monitoring," SPIE International Symposium on Smart Structures and Materials & Nondestructive Evaluation and Health Monitoring, Vol. 7292-56, (10 pages), March.

[2] A. Raghavan, and C. E. S. Cesnik, (2007), "Review of Guided-wave Structural Health Monitoring," The Shock and Vibration Digest, 39(2), 91-114.

[3] D. Zhou, D.S. Ha, and D.J. Inman, (2010), "Ultra Low-Power Active Wireless Sensor for Structural Health Monitoring," International Journal of Smart Structures and Systems, Vol. 6, No. 5-6, pp. 675-687, July/August.

[4] Kim, J., Grisso, B. L., Ha, D. S., and Inman, D. J., (2007), "An All-digital Low-power Structural Health Monitoring System". IEEE Conference on Technologies for Homeland Security, 123-8.

[5] Kim, J., Grisso, B. L., Ha, D. S., and Inman, D. J., (2007), "A System-On-Board approach for Impedance-based Structural Health Monitoring" Proceeding of SPIE, Vol. 6529, 65290O, San Diego, March.

[6] Wait, J.R., Park, G., Sohn, H. and Farrar, C.R., (2004), "Plate Damage Identification Using Wave Propagation and Impedance Methods," *Proc. of SPIE*, vol. 5394, pp. 53-65.

[7] Swartz, R.A., Flynn, E., Backman, D., Hundhausen, R.J. and Park, G., (2006), "Active Piezoelectric Sensing for Damage Identification in Honeycomb Aluminum Panels," *Proceedings of 24th Intl. Modal Analysis Conference.*

[8] S. Deyerle, D.S. Ha, and D.J. Inman, (2010), "A Low-Power System Design for Lamb Wave Methods," SPIE International Symposium on Smart Structures and Materials & Nondestructive Evaluation and Health Monitoring, Vol. 7650, 765019 (8 pages), March.

[9] J. G. Proakis, and D. G. Nanolakis, (2007) Digital Signal Processing, Prentice Hall.

[10] Park, S., Shin, H., and Yun, C., (2009), "Wireless impedance sensor nodes for functions of structural damage identification and sensor self-diagnosis", Smart Mater. Struct., 18- 055001.

[11] Park, S., Yun, C., Inman, D. J., and Park, G., (2008), "Wireless Structural Health Monitoring for Critical Members of Civil Infrastructures Using Piezoelectric Active Sensors", Proceeding of SPIE, Vol. 6935, 69350I, San Diego, March.

[12] Park, S., Lee, J., Yun, C., and Inman, D. J., (2008), "Electro-Mechanical Impedance-Based Wireless Structural Health Monitoring Using PCA-Data Compression and k-means Clustering Algorithms", Journal of Intelligent Material Systems and Structures, Vol. 19, No. 4, 509-520.

[13] Overly, T.G., Park, G., Farinholt, K.M., Farrar, C.R., (2008), "Development of an extremely compact impedance-based wireless sensing device," Smart Mat. and Struct., (17) 6: 065011.

[14] Mascarenas, D. L., Todd, M. D, Park, G. and Farrar, C. R., (2007), "Development of an impedance-based wireless sensor node for structural health monitoring" Smart Mater. Struct. (16) 6: 2137–2145.

[15] Taylor, S.G., Farinholt, K.M., Park, G. and Farrar C. R., (2009), "Impedance-Based Wireless Sensor Node for SHM, Sensor Diagnostics, and Low-Frequency Vibration Data Acquisition" Proc. of 7th International Workshop for Structural Health Monitoring, Palo Alto, CA, September.

[16] Park, G., Sohn, H., Farrar, C. R., and Inman, D. J., (2003), "Overview of piezoelectric impedance-based health monitoring and path forward", The Shock and Vibration Digest, 35, 451-463.

[17] Kim, Jina., (2007), "Low-Power System Design for Impedance-Based Structural Health Monitoring", PhD Dissertation, Virginia Tech.

[18] S. Legendre, D. Massicotte, J. Goyette et al, (2000), ""Wavelet-Transform-Based Method of Analysis for Lamb-Wave Ultrasonic NDE Signals," IEEE Trans. on Inst. and Meas., 49(3), 524-530.

[19] H. P. Sohn, W. G., J.R., N. P. Limback et al, (2004), "Wavelet-based active sensing for delamination detection in composite structures," Journal of Smart Materials and Structures, 13, 153-160.

[20] Yuxin Qin, Yijun Liang, Yinghao Zhang, Guang Zhang, (2010), "Experimental Study on an Optical Fiber Acoustic Emission Sensor Array" Academic Symposium on Optoelectronics and Microelectronics Technology and 10th Chinese-Russian Symposium on Laser Physics and Laser Technology.

[21] Ákos Lédeczi, Thomas Hay, Péter Völgyesi, D. Robert Hay, András Nádas, and Subash Jayaraman, (2009), "Wireless Acoustic Emission Sensor Network for Structural Monitoring" IEEE SENSORS JOURNAL, VOL. 9, NO. 11, NOVEMBER.

[22] R. K. Miller, (2006), "Acoustic emission testing," in *Nondestructive Testing Handbook*, 3rd ed. Columbus, OH: Amer. Society for Non-Destruc- tive Testing, vol. 6.

[23] www.pacndt.com

[24] www.aesensor.co.uk , www.vallen.de/products/sensors.htm

[25] TMS320F2812 Digital Signal Processor Data Manual, Texas Instruments Inc., May 2006.